CDF note 9683

Measurement of the Top Quark Mass with 2.7 fb^{-1} of CDF Run II Data in the Lepton+Jets Channel using only Leptons

The CDF Collaboration
URL http://www-cdf.fnal.gov
(Dated: July 27, 2009)

A measurement of the top quark mass using 2.7 fb^{-1} of CDF Run II Data is reported, which uses only the transverse momentum P_T of the leptons in the lepton+jets decay channel of top quark pairs and is therefore free of the uncertainties related with the measurement of the jet energy. The top quark mass M_{top} is measured with two methods: using the full shape of the lepton P_T distribution, which is the baseline or shape analysis method, and using only the mean value of the lepton P_T distribution, which is the cross-checking or $\langle P_T \rangle$ analysis method. M_{top} is measured from electrons and muons separately with either method and the results from the two lepton samples are combined in the end. The results are $\mathbf{(176.9 \pm 8.0_{stat} \pm 2.7_{syst})\ GeV/c^2}$ from the shape analysis method and $(178.7 \pm 8.1_{stat} \pm 3.2_{syst})$ GeV/c^2 from the $\langle P_T \rangle$ analysis method.

Preliminary Results for Winter 2003 Conferences

I. INTRODUCTION

This note describes a measurement of the top quark mass M_{top} using only leptons detected in the lepton+jets decay channel of $t\bar{t}$ pairs produced in $\bar{p}p$ collisions at $\sqrt{s} = 1.96$ TeV with the CDFII detector [1] at the Fermilab Tevatron. The measurement uses secondary vertex tagging for b-jet identification in order to reduce the background from W plus multijet production. The motivation for using only lepton (electron or muon) information to measure the top quark mass arises from the relatively large uncertainties associated with the jet calibration and the elaborate effort which is necessary for the jet calibration. The transverse momentum P_T of the muons or transverse energy E_T of the electrons from top quark decays, hereby generically refered to as the lepton P_T , is a variable which is free of these uncertainties and easy to implement. It is common to the semi-leptonic (or lepton+jets) and all-leptonic (or dilepton) decay channels of $t\bar{t}$ pairs and therefore allows for measurements of M_{top} in the two channels using the same method. It can be precisely calibrated using dilepton data from Z boson decays, where the kinematics is simple and the lepton P_T is well constrained by the precisely known Z boson mass. In addition, from a theoretical point of view, a measurement of M_{top} from the lepton P_T is ultimately free of the limit of $\Lambda_{QCD} \sim 300$ MeV/c^2 in the precision of any measurement of M_{top} using jets, which is imposed by parton fragmentation.

II. DATA SAMPLE & EVENT SELECTION

This analysis is based on data collected with the CDFII detector between March 2002 and April 2008. The data are collected with an inclusive lepton trigger that requires an electron with E_T >18 GeV or muon with P_T >18 GeV/c. From this inclusive lepton dataset events are selected offline by requiring one and only one reconstructed isolated central lepton (with pseudo-rapidity $|\eta| \leq 1$), either electron with E_T >20 GeV or muon with P_T >20 GeV/c, at least four central jets (with $|\eta| \leq 2$) having E_T >20 GeV and missing transverse energy $\not\!\!E_T > 20$ GeV. The dataset thus selected, called "lepton+$\geq$ 4jets", is dominated by QCD production of W bosons with multiple jets. To improve the signal-to-background (S/B) ratio, events with at least one b-jet are identified by requiring at least one secondary vertex tag. The "b-tagging" cut, having an efficiency of 40%, enhances the S/B ratio to 3.2 for the electrons and 4.5 for the muons. Good runs with the silicon vertex detector on are also required for the b-tagging. 472 electrons and 386 muons are thus selected from a data sample corresponding to an integrated luminosity of 2.7 fb^{-1}.

In the Monte Carlo, the Pythia 6.216 generator [2] is used for the $t\bar{t}$ signal samples and the Alpgen 210′ [3] + Pythia generator (Pythia here for parton showering only) is used for the background samples.

III. BACKGROUNDS

A model for the expected background in the lepton+$\geq$ 4jets data sample is built by a standard fit, called "Method II", also used for the measurement of the cross section for $t\bar{t}$ production in the lepton+jets decay channel [4]. Background contributions are expected from QCD production of W and Z bosons associated with jets, single top (electroweak) production and "fake" leptons, i.e. jets mis-identified as leptons. Background lepton P_T distributions from W boson production associated with heavy flavor (c, b) jets, Z boson production associated with light flavor jets, diboson (WW, WZ, ZZ) production and single top production are modeled by the Monte Carlo (MC). The shape of the background lepton P_T distribution from W boson production associated with light flavor (u, d, s) jets is modeled by the MC and its magnitude is etimated from the negative b-tag rate (mistags). The shape of the background distribution of fake leptons is determined from the data by selecting leptons with one of the cuts required for the definition of a tight lepton inverted. The leptons thus selected are refered to as "anti-leptons". Finally, the magnitude of the fakes background is estimated by a fit to the $\not\!\!E_T$ spectrum of the data, varying the amount of fakes and keeping all of the other background components fixed. The fit gives 112 ± 29 expected background electrons and 71 ± 9 expected background muons in the data sample of 2.7 fb^{-1}. The expected fake electrons are 40 ± 10 and the expected fake muons are 0 ± 1.

The procedure for building the background model in the $\geq$ 4-jets multiplicity bin is repeated in the 1-jet bin, where the signal from top quarks is negligible and the model histograms can be tested against real data (control region). Figures 1 and 2 show the background models in the signal region and the comparison of the corresponding models with the data in the control region. The bin-by-bin ratios of the data histograms to the model histograms in the control region are flat and consistent with unity, providing thus confidence for the expected background models in the signal region.

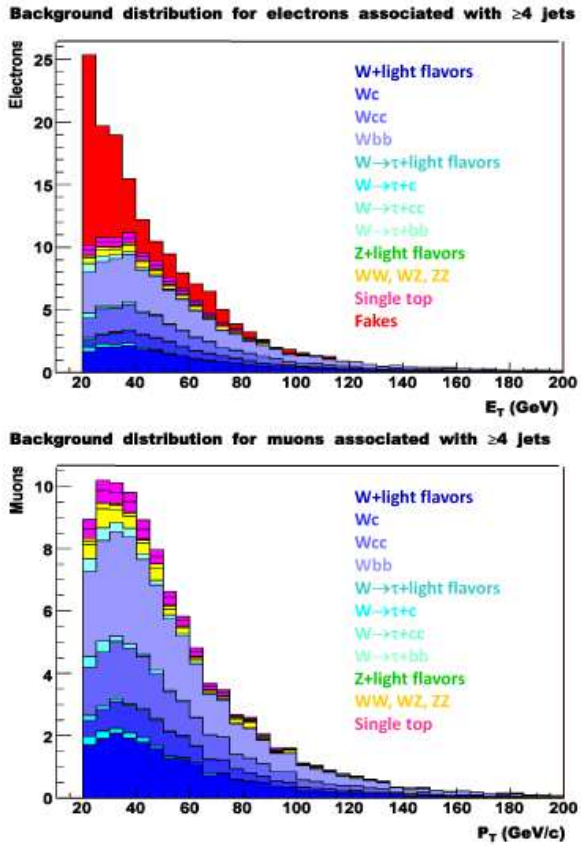

FIG. 1: The background models in the $\geq$ 4-jets signal bin.

IV. SENSITIVITY OF THE LEPTON P_T TO THE TOP QUARK MASS

Figure 3 shows the dependence of the mean value $\langle P_T \rangle$ of the lepton P_T on M_{top} for electrons and muons separately. The dependence is linear within MC statistics. The slope of $\langle P_T \rangle$ vs. M_{top} is about 13% in either case. This simple relation between $\langle P_T \rangle$ and M_{top} allows for a straightforward measurement of M_{top} from $\langle P_T \rangle$ of a given lepton sample:

$$M_{top} = \frac{\langle P_T \rangle - \kappa}{\lambda} \qquad (\delta M_{top})_{stat} = \frac{1}{\lambda} \times \frac{P_T^{rms}}{\sqrt{N}} \tag{1}$$

where κ is the intercept and λ the slope of $\langle P_T \rangle$ vs. M_{top} , P_T^{rms} is the second moment of the distribution and N is the total number of leptons in the sample. This method is simple and therefore useful for cross-checking and understanding, but makes limited use of the information provided by the lepton P_T spectrum and is sensitive to the composition of the lepton sample or, equivalently, to the background normalization.

The full shape of the lepton P_T distribution can be accurately parameterized by an incomplete Γ function with two free parameters, the expected number p of leptons per measurement and the expected average P_T per lepton q:

$$F(P_T) = \frac{1/q}{\Gamma(1+p, c/q)} \left(\frac{P_T}{q}\right)^p e^{-P_T/q} \times \frac{1}{1+e^{(c-P_T)/a}} \qquad a,\ c,\ p,\ q > 0 \tag{2}$$

The Fermi distribution factor on the right hand side models the cut at c=20 GeV/c with a fixed steepness parameter a=0.1 GeV/c. Figure 4 shows that the dependence of p and q on M_{top} is again linear within MC statistics. The parameter p shows a very weak, but still significant, dependence on M_{top} with a slope of about -0.5%, whereas q is much more sensitive to M_{top} with a slope of about 10%.

M_{top} can therefore be alternatively measured by maximizing the unbinned likelihood function

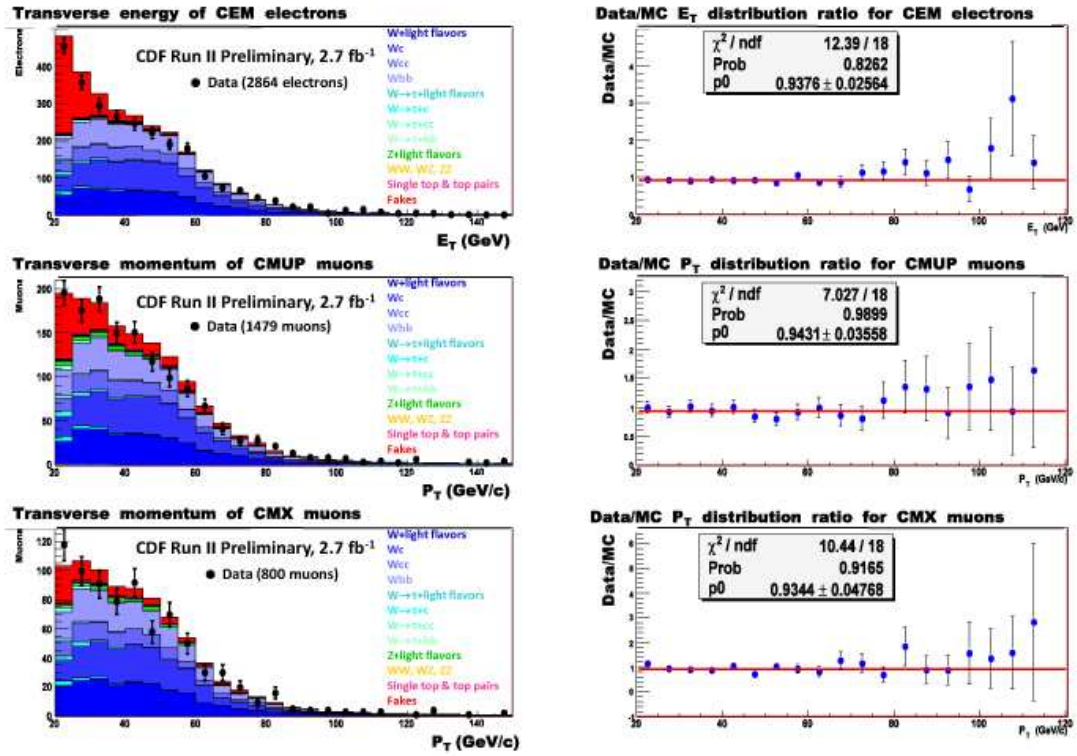

FIG. 2: **Left:** Comparison of data and MC in the 1-jet control bin. **Right:** Data-to-MC ratios in the 1-jet control bin. CEM are central electrons and CMUP, CMX are two categories of central muons.

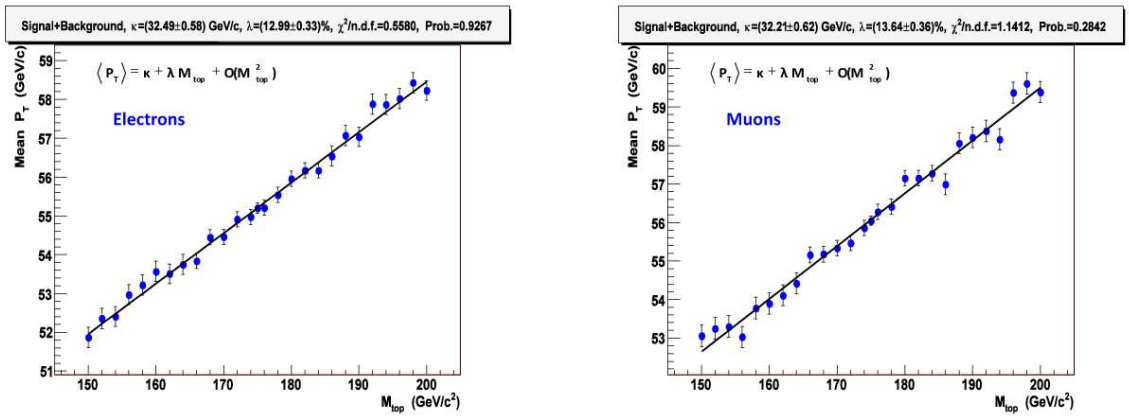

FIG. 3: The mean of the MC P_T distribution of the electrons (left) and of the muons (right) for signal+background as a function of the top quark mass.

$$L = L_B \times L_{shape} \tag{3}$$

$$L_B = \frac{1}{\sqrt{2\pi}\,\delta B} \exp\left[-\frac{1}{2}\left(\frac{k-B}{\delta B}\right)^2\right] \tag{4}$$

$$L_{shape} = \frac{(j+k)^N e^{-(j+k)}}{N!} \prod_{i=1}^{N} \frac{j \times F_{sig}\left(P_T^{(i)};\, \tilde{\alpha};\, M_{top}\right) + k \times F_{bg}\left(P_T^{(i)};\, p_{bg}\,,\, q_{bg}\right)}{j+k} \tag{5}$$

which depends on M_{top} through

$$p_{sig} = \alpha_1 + \alpha_2 M_{top} \qquad q_{sig} = \alpha_3 + \alpha_4 M_{top} \tag{6}$$

L is maximized with respect to M_{top} , the number of signal leptons j and the number of background leptons k, keeping the total number N of leptons in the sample and the shape parameters $\vec{\alpha} = (\alpha_1\,,\ \alpha_2\,,\ \alpha_3\,,\ \alpha_4)$ of the signal distribution and $(p_{bg}\,,\ q_{bg})$ of the background distribution fixed. This method makes full use of the information provided by the lepton P_T spectrum. In addition, the dependence on the background normalization is marginalized through the gaussian constraint L_B on the expected number $B \pm \delta B$ of background leptons.

V. CORRECTIONS TO THE MEASURED TOP QUARK MASS

For the lepton P_T calibration, the global scale is first calibrated using $Z \to e^+e^-$ and $Z \to \mu^+\mu^-$ data and MC. The dilepton invariant mass is recontsructed from this data and its spectrum is fit with a function to accurately determine the centroid, which is then compared with the world average of the Z boson mass. The comparison provides a global correction to the lepton P_T . For the local scale, non-linear corrections for the spectrometer response are studied using $Z \to \mu^+\mu^-$ data. $1/P_T$ is binned and the di-muon invariant mass is reconstructed in each bin and tuned to the world average of the Z boson mass. This provides a local correction to the lepton P_T . Having the momentum calibrated with the di-muon sample, non-linear corrections for the calorimeter response, related with the measurement of the transverse energy of the electrons, are studied using electron+1jet data. This sample is dominated by W boson decays associated with one jet. The transverse energy E_T of the electrons is binned and the ratio E/P of the energy to the momentum of the electrons, corrected for the momentum calibration, is integrated over each bin. The fraction of integrated E/P of the data over integrated E/P of the MC is studied as a function of E_T for each bin. Non-linear corrections to the electron E_T spectrum are derived from the slope of this fraction with respect to E_T . The global and local P_T scale corrections are then applied to the measurement of M_{top} .

For the parton distribution functions (PDF) the Pythia MC is re-weighted from the leading order (LO) default set CTEQ5L to the next-to-leading order (NLO) set CTEQ6M and the LO 5% fraction of $t\bar{t}$ events that Pythia produces via gluon-gluon fusion is also re-weighted to the NLO fraction of 10%.

Finally, in the $\langle P_T \rangle$ analysis method, a $+(0.8 \pm 0.3)$ GeV/c^2 bias in the mass measurement from the electron sample and a $+(1.4 \pm 0.3)$ GeV/c^2 bias in the mass measurement from the muon sample, detected in the mass residuals of pseudo-experiments, are also corrected.

All corrections applied to the measured M_{top} are summarized in Table I.

	Electrons		Muons	
Correction (in GeV/c^2)	$\langle P_T \rangle$ analysis	Shape analysis	$\langle P_T \rangle$ analysis	Shape analysis
Global P_T scale	+2.59	+2.55	+0.57	+0.57
Local P_T scale	+1.23	+1.19	+1.71	+1.69
PDF	+2.40	+2.55	+2.30	+2.35
Bias	+0.82	–	+1.43	–
Total	+7.04	+6.29	+6.01	+4.61

TABLE I: Corrections applied to the measured top quark mass.

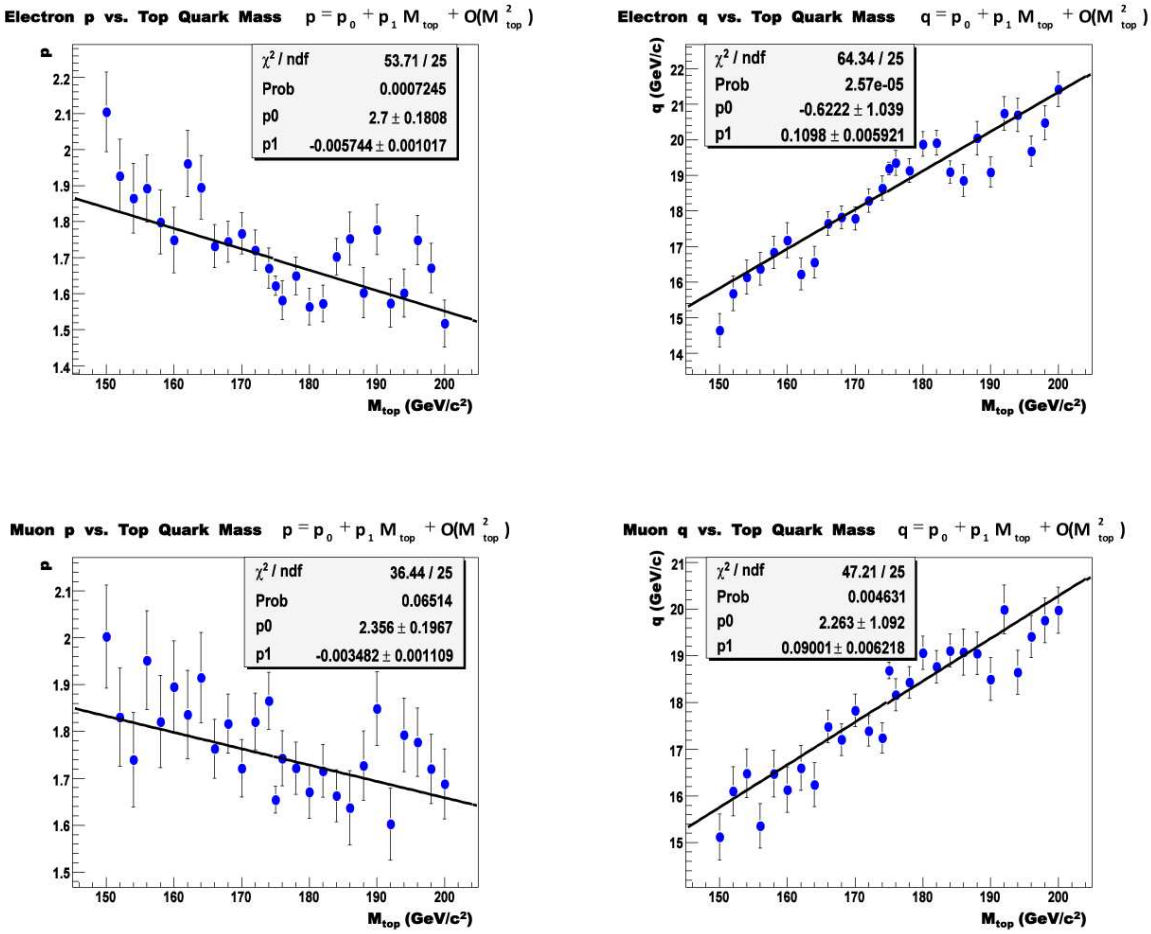

FIG. 4: The dependence of the shape parameters of the MC P_T distribution on the top quark mass for the electrons (top) and for the muons (bottom).

VI. SYSTEMATIC UNCERTAINTIES

- The uncertainty from the finite MC statistics is estimated by varying the $\langle P_T \rangle$ or shape parameters, according to the M_{top} measurement method, by $\pm 1\sigma$ about their central values determined from the fits to the MC templates, taking into account the total anti-correlation of intercept and slope with respect to M_{top} (see Section IV).
- The uncertainty from the global P_T scale calibration is estimated by varying the global P_T scale correction coefficient by $\pm 1\sigma$ about its central values determined from the fits to the dilepton data and MC (see Section V).
- The uncertainty from the local P_T scale calibration is estimated by varying the local P_T scale correction coefficients by $\pm 1\sigma$ about their central values determined from the fits to the di-muon data (for the muons) and the e+1jet data (for the electrons), taking into account the total anti-correlation of intercept and slope with respect to P_T (see Section V).
- The uncertainty from the MC generator is estimated by comparing two different generators for the signal, Pythia and Herwig [5], adding in both cases the same background. The difference between the two results is taken as $\pm 1\sigma$ and the uncertainty is defined as $\pm 1\sigma$.
- The uncertainty from the initial/final state radiation (IFSR) of gluons is estimated by varying the radiation strength in Pythia by an amount appropriately tuned to various data sets.

- The uncertainty associated with the PDF re-weighting in the Pythia MC is estimated from the mass shifts of the 20 CTEQ6M eigenvectors from the mass measurement with the nominal CTEQ6M set and the shift of the average of 6 α_S values from the world average of $\alpha_S(M_Z)$, all added in quadrature.
- The uncertainty from the choice of the Q^2 scale in the W+jets MC background is estimated by varyying the scale by a factor of 2.0 and 0.5 of the default.
- The uncertainty from the jet energy scale (JES) is estimatedby varying the jet energy scale by $\pm 1\sigma$ of the combined jet energy corrections.
- The uncertainty from event pile-up is estimated by re-weighting the average number of vertices in the MC (1.5) to the average number of vertices in the data after the first 1.2 fb^{-1} (2.0).
- The uncertainty from the fake electrons, which affects the shape of the background P_T distribution by changing the composition of the background sample, is estimated by varying the amount of anti-electrons in the background model by $\pm 25\%$ (the corresponding Method II fit uncertainty, see Section III).
- The uncertainty due to the overall normalization of the background in the $\langle P_T \rangle$ analysis method is estimated by varying the total amount of background by the respective Method II fit uncertainty ($\pm 25\%$ for the electrons, $\pm 15\%$ for the muons, see Section III).
- The uncertainty from the bias correction in the $\langle P_T \rangle$ analysis method is ± 0.3 GeV/c^2, as determined from the pseudo-experiments.

The systematic uncertainties are summarized in Tables II and III. They are assumed to be totally uncorrelated in the electron and muon samples when they are estimated from statistically independent samples or when at least one systematic shift is smaller than the associated statistical uncertainty. Otherwise they are assumed totally correlated.

	Electrons		Muons		
Source	$\langle P_T \rangle$ analysis (GeV/c^2)	Shape analysis (GeV/c^2)	$\langle P_T \rangle$ analysis (GeV/c^2)	Shape analysis (GeV/c^2)	Correlation
MC statistics	± 0.3	± 0.4	± 0.3	± 0.4	0
Global P_T scale	± 0.2	± 0.2	± 0.1	± 0.1	0
Local P_T scale	± 0.6	± 0.6	± 1.5	± 1.5	1
Generator	± 0.7	± 0.7	± 2.2	± 2.2	0
IFSR	± 1.5	± 1.5	± 0.7	± 0.7	0
PDF	± 0.5	± 0.6	± 0.5	± 0.6	1
Q^2	± 0.7	± 0.7	± 0.8	± 0.8	0
JES	± 0.0	± 0.0	± 0.0	± 0.0	1
Multiple Interactions	± 0.1	± 0.1	± 0.1	± 0.1	1
Fakes	± 3.8	± 3.6	–	–	0
Background	± 3.0	–	± 0.9	–	0
Bias correction	± 0.3	–	± 0.3	–	0
Total	± 5.2	± 4.1	± 3.1	± 3.0	

TABLE II: Top quark mass systematic error breakdown for each lepton sample, electrons or muons, and each measurement method.

VII. RESULTS

Figure 5 shows the unbinned maximum likelihood fits to the data and the respective log-likelihood curves. Figure 5 shows the sum of the two fits: background and total expectations provided by the two fits, logarithms of the likelihoods and data samples are added together for electrons and muons in this Figure. Table IV summarizes all of the top quark mass measurements from each lepton sample, electrons and muons, and each method, $\langle P_T \rangle$ analysis and shape analysis, before and after all corrections are applied.

The M_{top} measurements and the associated statistical and systematic errors from each lepton sample, electrons or muons, using one method, $\langle P_T \rangle$ analysis or shape analysis, are combined with the Best Linear Unbiased Estimator (BLUE) algorithm [6], in an iterative mode that accounts for the correlations between the respective uncertainties.

Source	$\langle P_T \rangle$ analysis (GeV/c^2)	Shape analysis (GeV/c^2)
MC statistics	±0.2	±0.3
Global P_T scale	±0.1	±0.1
Local P_T scale	±1.1	±1.1
Generator	±1.2	±1.2
IFSR	±0.8	±0.8
PDF	±0.5	±0.6
Q^2	±0.5	±0.5
JES	±0.0	±0.0
Mutiple Interactions	±0.1	±0.1
Fakes	±1.8	±1.8
Background	±1.8	–
Bias correction	±0.2	–
Total	±3.2	±2.7

TABLE III: Top quark mass systematic error breakdown for the combined measurements from electrons and muons with each method.

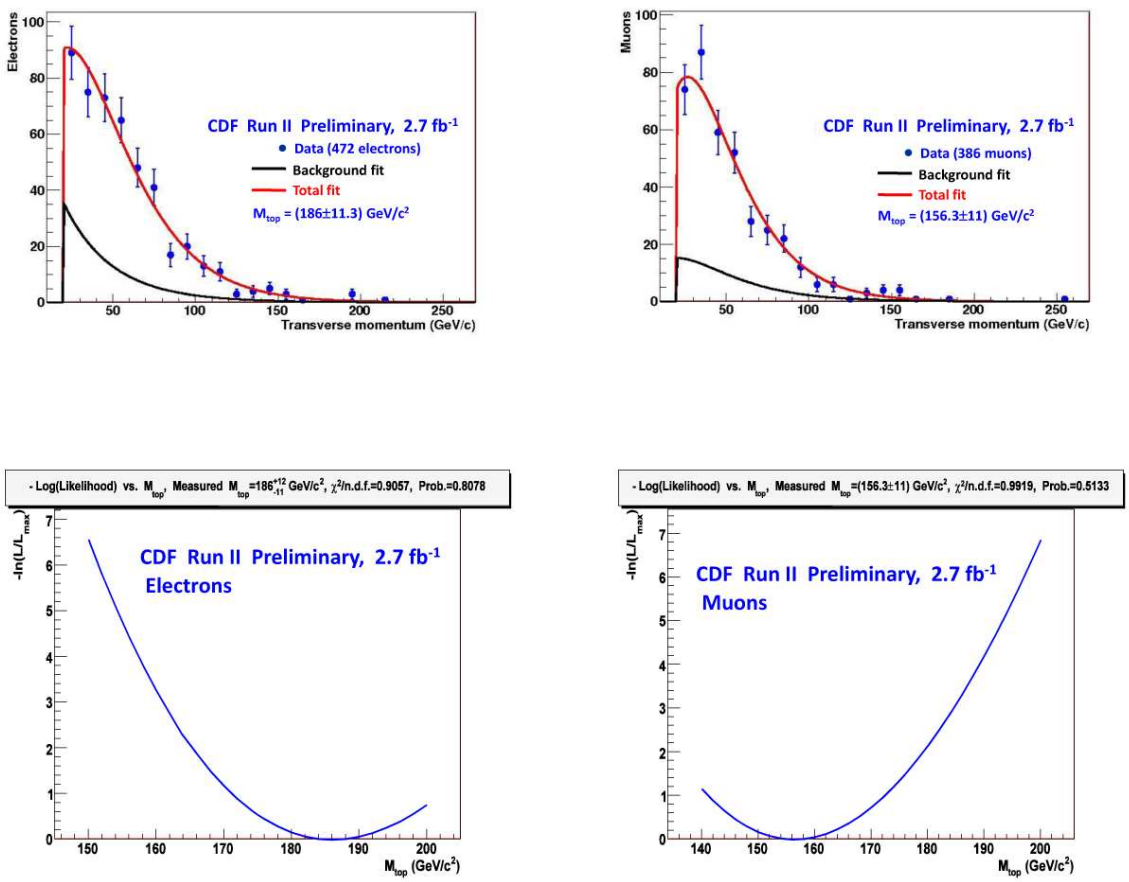

FIG. 5: **Top:** The unbinned maximum likelihood fits (red) to the data (blue) and the background expectations (black) provided by the fits. **Bottom:** The corresponding log-likelihood curves.

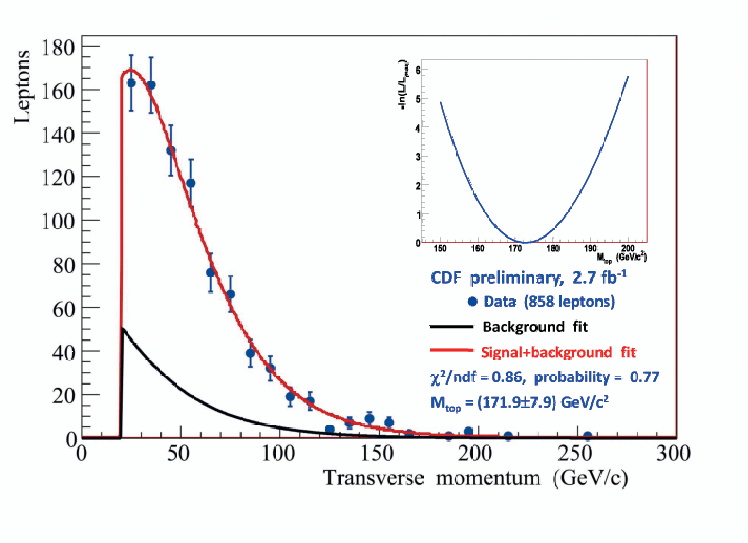

FIG. 6: The sum of the unbinned maximum likelihood fits for the two lepton samples (red) and the sum of the background expectations (black) compared with the data summed for electrons and muons (blue). The inset shows the sum of the corresponding log-likelihood curves.

	Electrons	
Measurement	$\langle P_T \rangle$ analysis (GeV/c^2)	Shape analysis (GeV/c^2)
Uncorrected	187.6±11.1	186.1±11.3
Corrected	194.6±11.1	192.4±11.3
	Muons	
Measurement	$\langle P_T \rangle$ analysis (GeV/c^2)	Shape analysis (GeV/c^2)
Uncorrected	157.3±11.3	156.3±11.0
Corrected	163.3±11.3	160.9±11.0

TABLE IV: Summary of all top quark mass measurements. The errors are statistical only.

The statistical uncertainties are assumed totally uncorrelated. The result from the combination of the measurements using the baseline shape analysis method is

$$\mathbf{M_{top} = (176.9 \pm 8.0_{stat} \pm 2.7_{syst})\ GeV/c^2}$$

The corresponding result from the cross-checking $\langle P_T \rangle$ analysis method is $(178.7 \pm 8.1_{stat} \pm 3.2_{syst})$ GeV/c^2. The two results are fully consistent within errors. They are also consistent with the current world average of $M_{top}^{world} = (173.1 \pm 0.6_{stat} \pm 1.1_{syst})$ GeV/c^2 [7].

[1] F. Abe, et al., Nucl. Instrum. Methods Phys. Res. A **271**, 387 (1988); D. Amidei, et al., Nucl. Instum. Methods Phys. Res. A **350**, 73 (1994); F. Abe, et al., Phys. Rev. D **52**, 4784 (1995); P. Azzi, et al., Nucl. Instrum. Methods Phys. Res. A **360**, 137 (1995); The CDFII Detector Technical Design Report, Fermilab-Pub-96/390-E

[2] Torbjörn Sjöstrand, Leif Lönnblad, Stephen Mrenna, "Pythia 6.2 physics and manual", hep-ph/0108264v1; T. Sjostrand et al., High-Energy-Physics Event Generation with PYTHIA 6.1, Comput. Phys. Commun. **135**, 238 (2001).

[3] M.L. Mangano, M. Moretti, F. Piccinini, R. Pittau, A.D. Polosa, "ALPGEN, a generator for hard multiparton processes in hadron collisions", hep-ph/0206293.

[4] CDF Collaboration, "Measurement of the Top Quark Pair Cross Section in the Lepton+Jets Decay Channel with 2.7 fb^{-1}", Conference Note 9462.

[5] G. Corcella et al., HERWIG 6: An Event Generator for Hadron Emission Reactions with Interfering Gluons (including supersymmetric processes), JHEP **01**, 10 (2001).
[6] L. Lyons *et al*, *Nucl. Inst. Meth. A*, **270**, 110 (1988); *Phys. Rev. D*, **3**, 982 (1990); A. Valassi, *Nucl. Inst. Meth. A*, **500**, 391 (2003).
[7] The Tevatron Electroweak Working Group for the CDF and D0 Collaborations, "Combination of CDF and D0 Results on the Mass of the Top Quark", FERMILAB-TM-2427-E, March 2009.